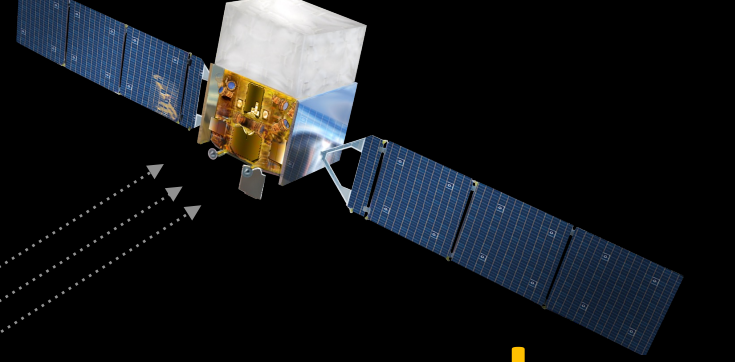

Light at the end of the tunnel:
Astrophysical searches for axion-like particles in gamma-ray energies

TeVPA 2022
Queen's Univiersity
August 10, 2022

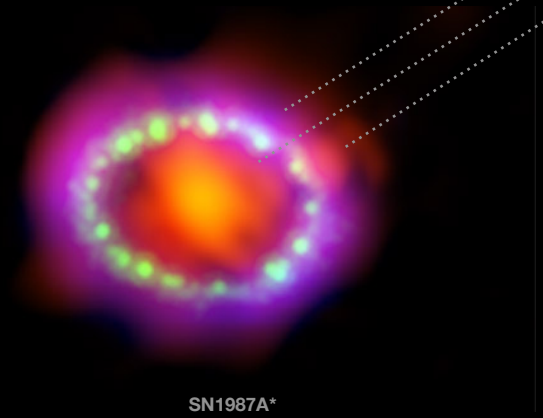

Milena Crnogorčević
University of Maryland/NASA Goddard
mcrnogor@umd.edu

*Credit: X-ray: NASA/CXC/SAO/PSU/K.Frank et al.; Optical: NASA/STScI; Millimeter: ESO/NAOJ/NRAO/ALMA

TODAY:

- Axion-like particles: Introduction and motivation
  1. *Fermi*-LAT Low Energy Technique: Sensitivity study
  2. Sensitivity of the future MeV instruments
  3. Gamma-ray Bursts as ALP factories: what has *Fermi* seen so far?
- Sneak peak: GRB precursors and ALPs

WHAT ARE AXION-LIKE PARTICLES? (ALPs)

- Extension of the axion, a proposed solution of the strong charge-parity problem in QCD

- WISPs: weakly-interacting sub-eV particles (mass $\lesssim 10^{-10}$ eV)

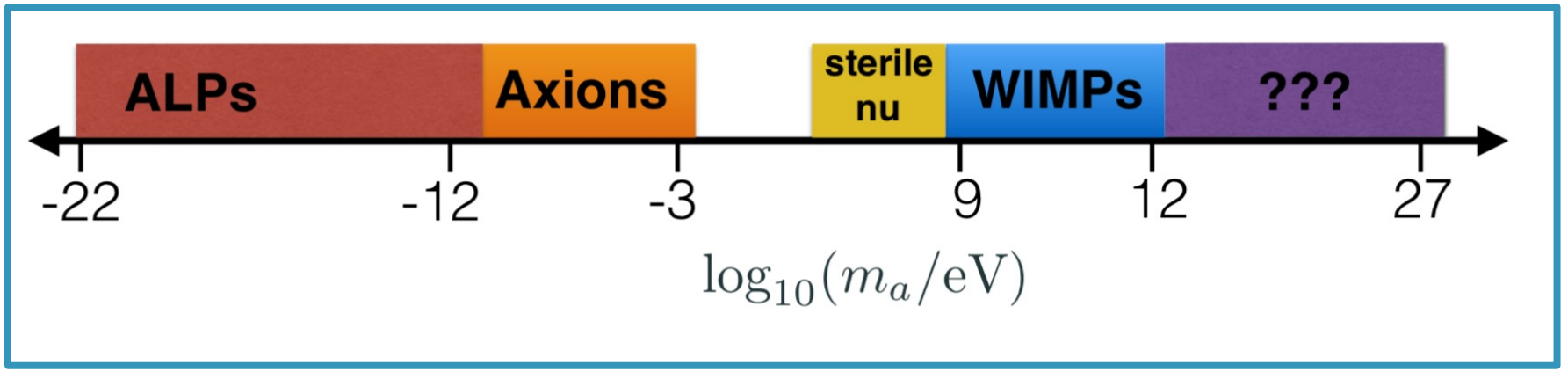

WHAT ARE AXION-LIKE PARTICLES? (ALPs)

- Extension of the axion, a proposed solution of the strong charge-parity problem in QCD

- WISPs: weakly-interacting sub-eV particles (mass $\lesssim 10^{-10}$ eV)

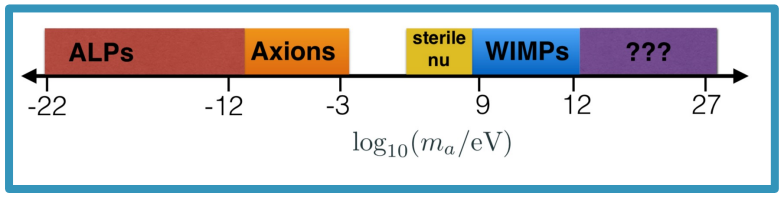

- Cold matter requirements:
  - ✓ feeble interactions with standard model particles
  - ✓ cosmological stability

- Direct and indirect searches → limits on coupling/mass parameter space

- **Non-thermal** production of ALPs via *misalignment mechanism* or inverse *Primakoff process*

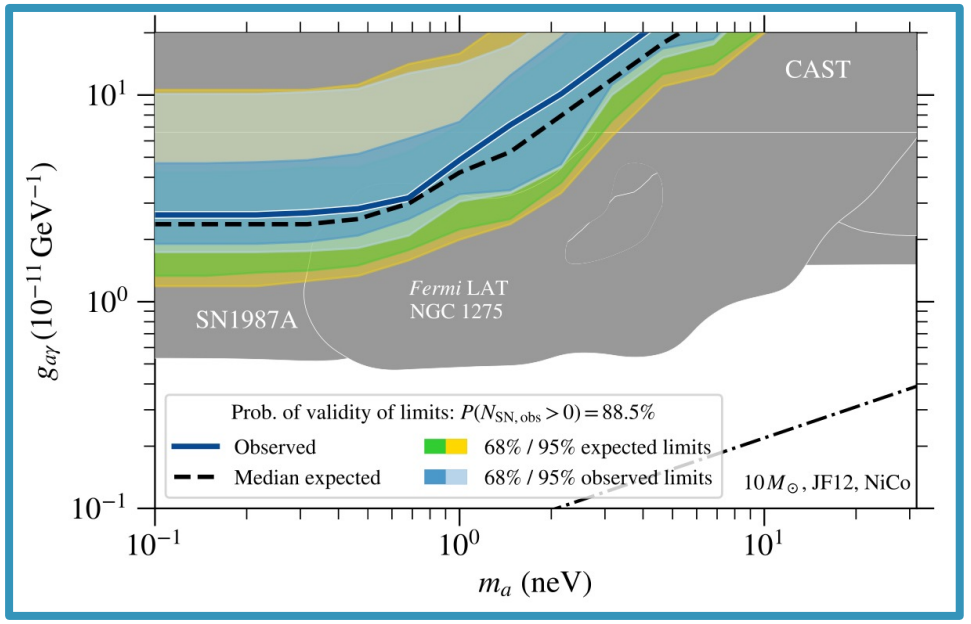

Exclusion plot for ALPs. [Meyer & Petrushevska 2020]

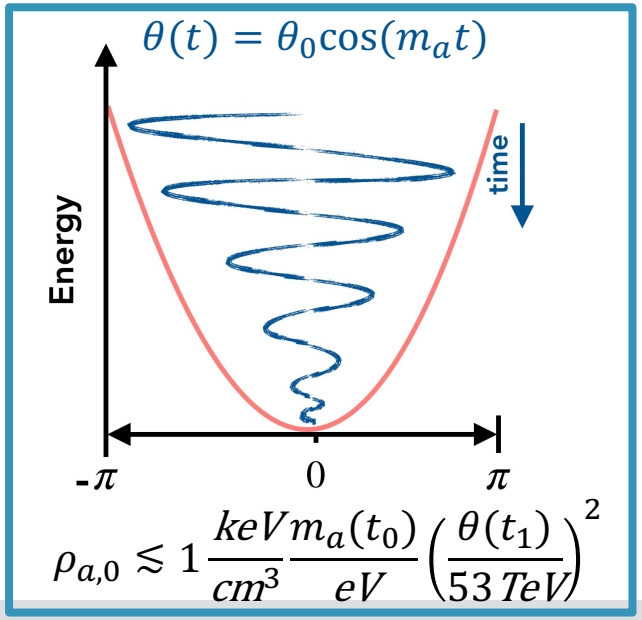

OBSERVING ALPs WITH GAMMA-RAYS

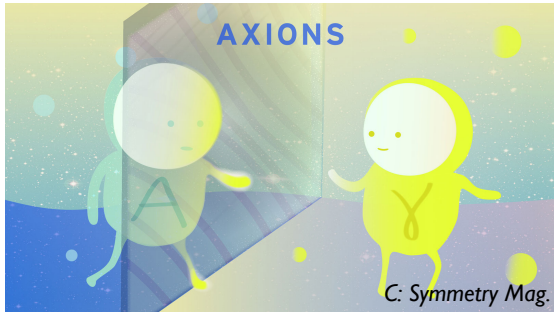

- **Primakoff process:** converting ALPs into photons

- In the presence of an external magnetic field, **B**, ALPs undergo a conversion into gamma-rays:

$$\mathcal{L}_{a\gamma\gamma} \supset -\frac{1}{4} g_{a\gamma\gamma}\, \mathbf{E} \cdot \mathbf{B}\, a$$

where $g_{a\gamma}$ is ALP-photon coupling rate, and a is the axion field strength.

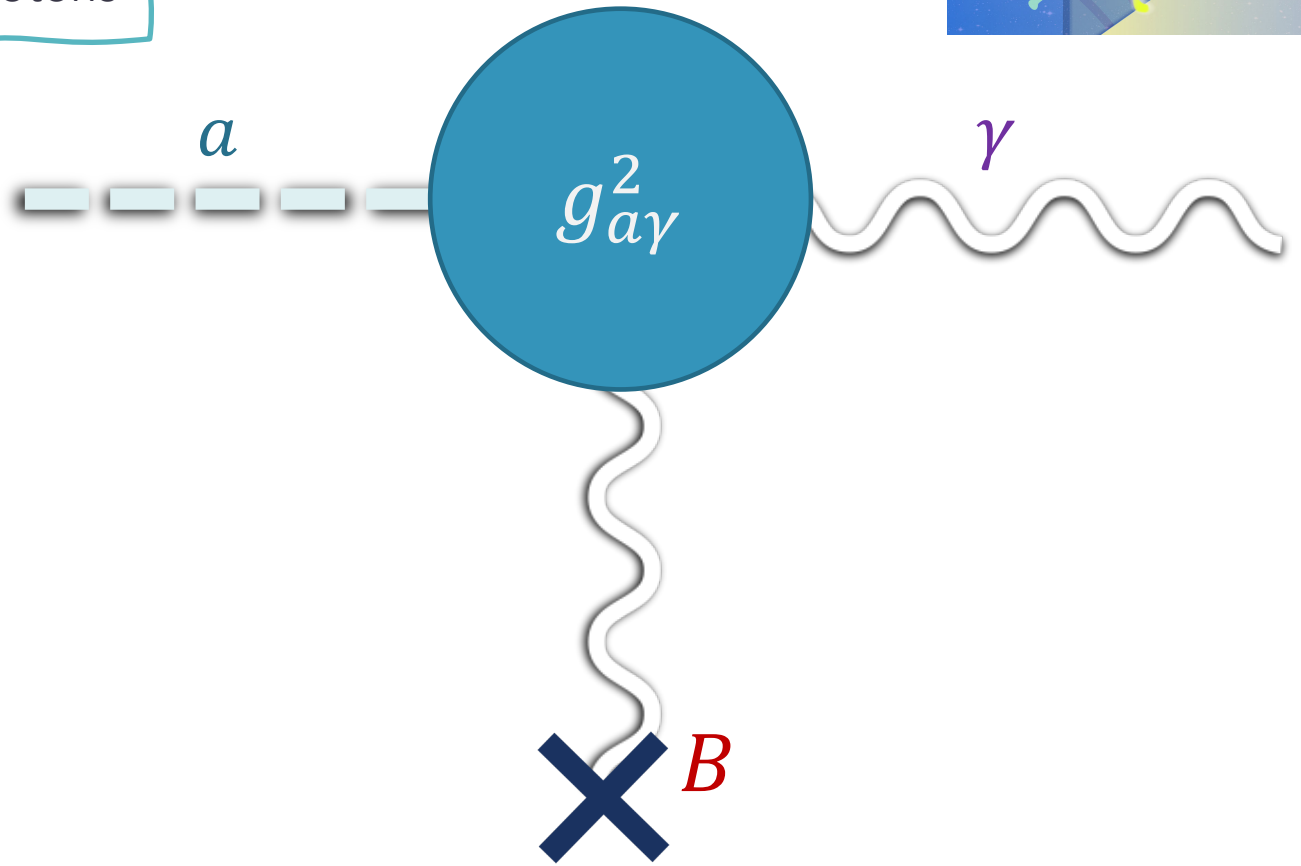

[e.g. Raffelt & Stodoslky 1988]

OBSERVING ALPs WITH GAMMA-RAYS

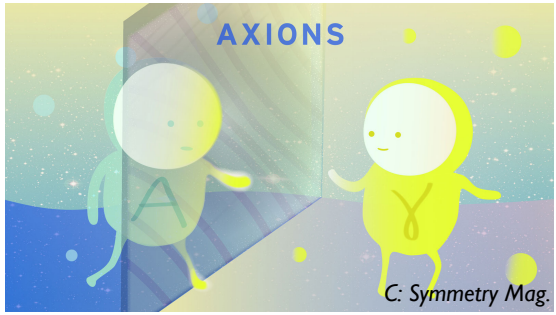

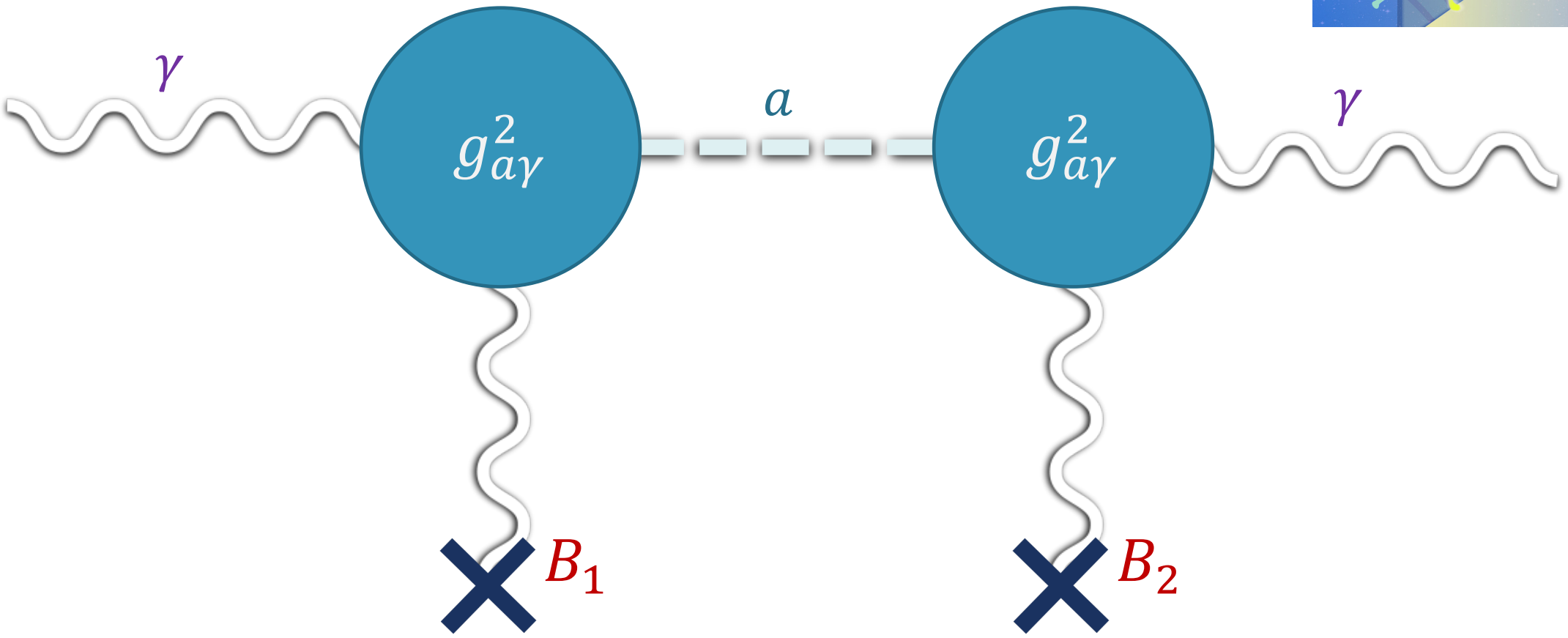

(production: Primakoff effect)

(detection: inverse Primakoff effect)

[e.g. Raffelt & Stodolsky 1988]

TAKE-AWAY POINTS ABOUT ALPs

- Viable *cold* dark-matter candidate, belonging to the family of WISPs (weakly-interacting *sub*-eV particles)
- ALPs convert into photons in the presence of a magnetic field (inverse Primakoff process)
- Gamma-ray observations can probe ALP parameter space

TAKE-AWAY POINTS ABOUT ALPs

- Viable *cold* dark-matter candidate, belonging to the family of WISPs (weakly-interacting *sub-eV* particles)
- ALPs convert into photons in the presence of a magnetic field (inverse Primakoff process)
- Gamma-ray observations can probe ALP parameter space

TAKE-AWAY POINTS ABOUT ALPs

- Viable *cold* dark-matter candidate, belonging to the family of WISPs (weakly-interacting *sub-eV* particles)
- ALPs convert into photons in the presence of a magnetic field (inverse Primakoff process)
- Gamma-ray observations can probe ALP parameter space

TAKE-AWAY POINTS ABOUT ALPs

- Viable *cold* dark-matter candidate, belonging to the family of WISPs (weakly-interacting *sub-eV* particles)
- ALPs convert into photons in the presence of a magnetic field (inverse Primakoff process)
- Gamma-ray observations can probe ALP parameter space

HOW FAR CAN FERMI SEE?

Axion-like Particles from Core-collapse Supernovae: Investigating *Fermi* Sensitivity with the LAT Low-energy Technique

Crnogorčević et al. 2021 (PRD, arXiv:2109.05790)

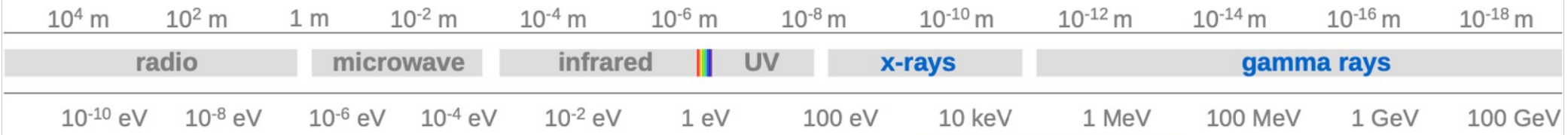

GBM Gamma-ray Burst Monitor

12 (NaI) + 2 (BGO) detectors
FoV: entire unocculted sky
8 keV to 40 MeV
~1500 bursts (~1 every day or two)

LAT Large Area Telescope

Pair-production telescope
FoV: 2.4 sr (~20% of sky)
20 MeV to >300 GeV

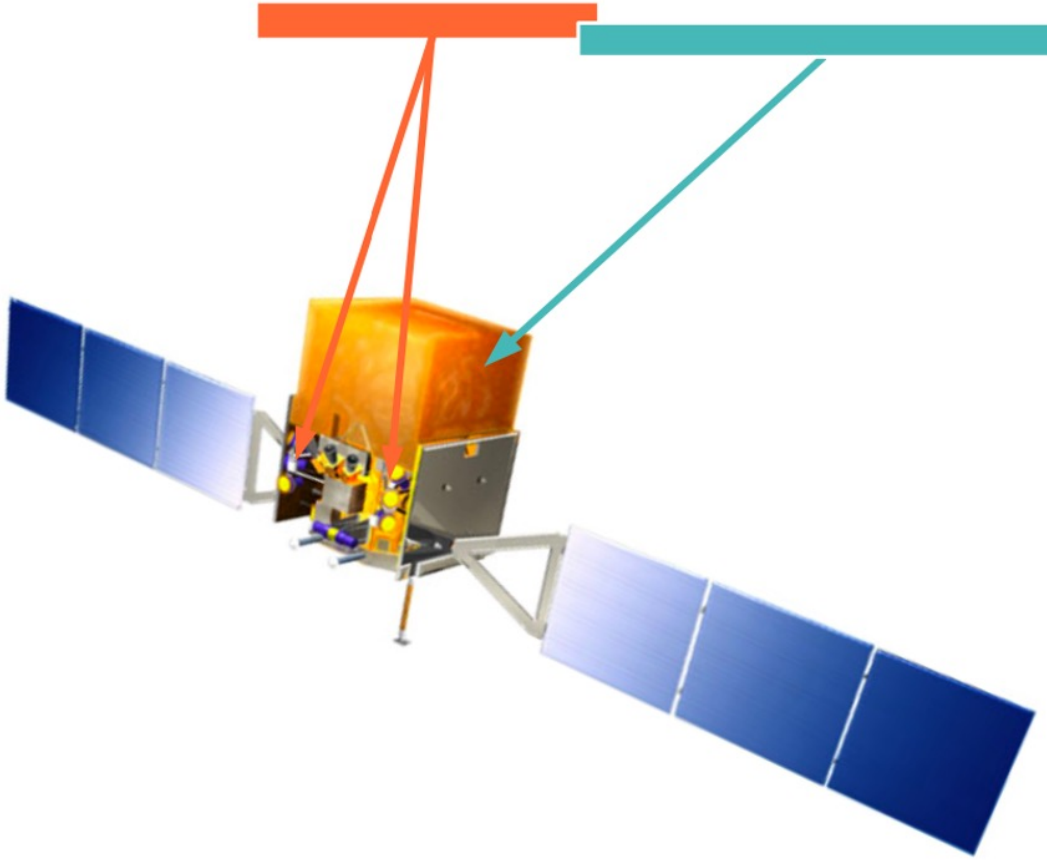

MOTIVATION AND ASSUMPTIONS

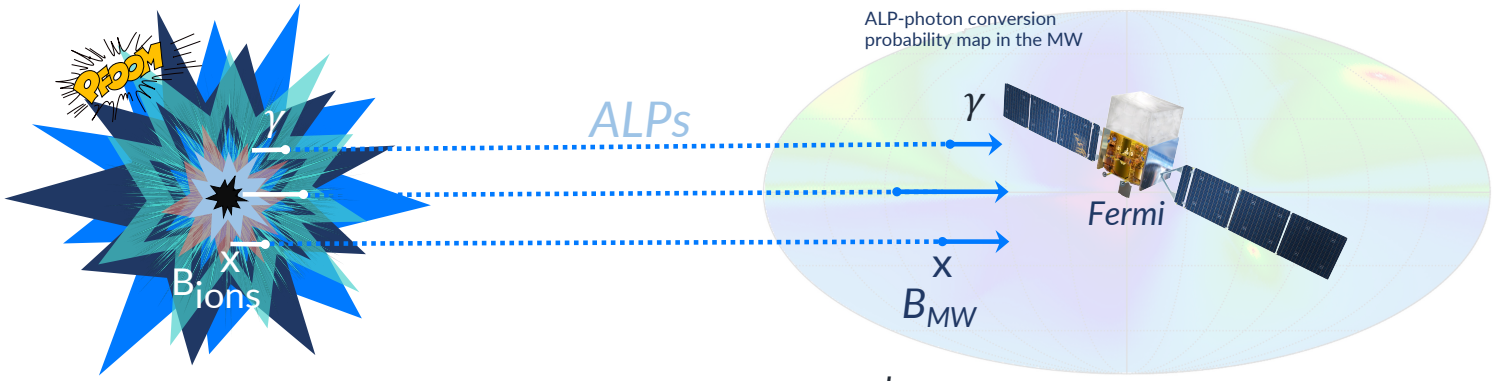

Primakoff Process inside the CCSN core

Inverse Primakoff Process in the MW B-field

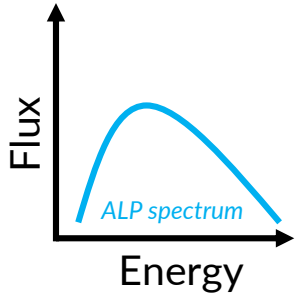

MOTIVATION AND ASSUMPTIONS

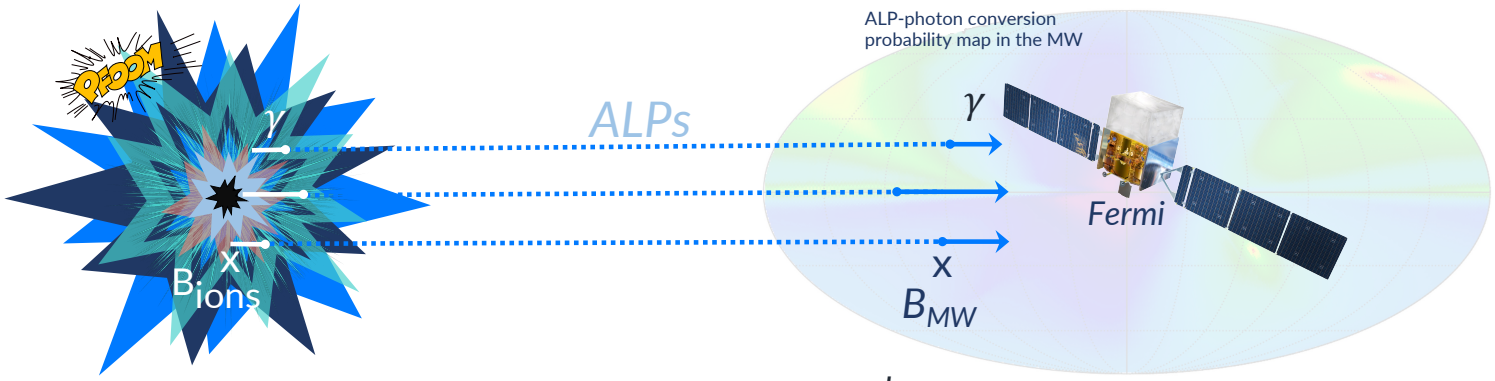

Primakoff Process inside the CCSN core

Inverse Primakoff Process in the MW B-field

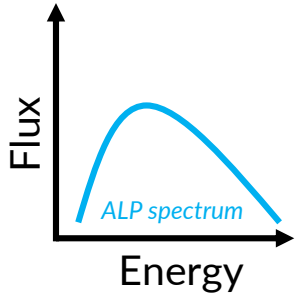

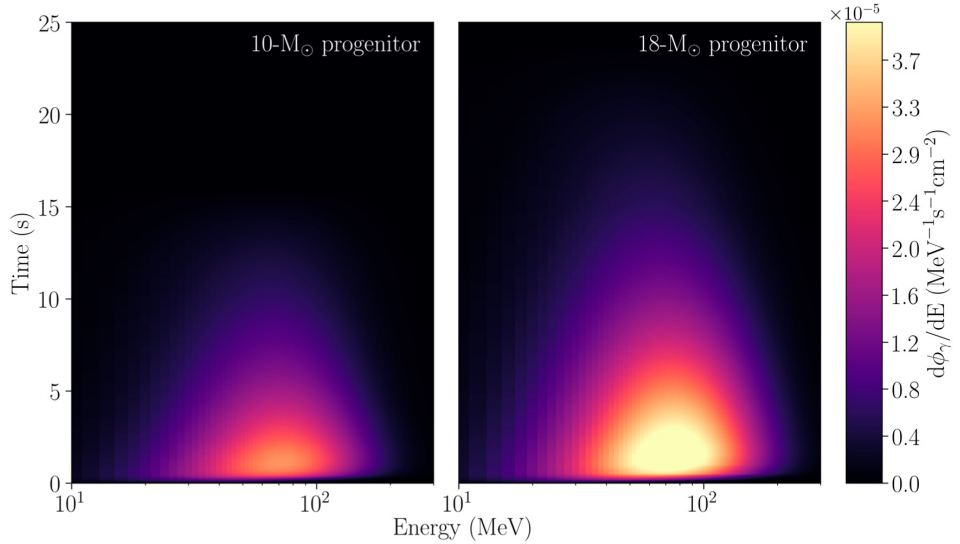

Observed evolution of the ALP-induced gamma-ray emission in time and energy in a core-collapse of a 10 and 18-M⊙ progenitor.

MOTIVATION AND ASSUMPTIONS

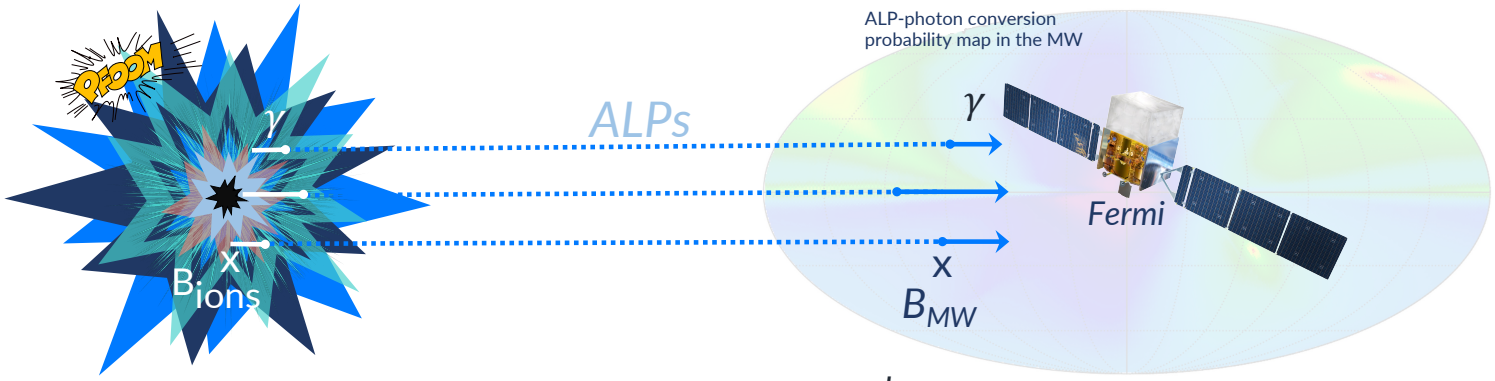

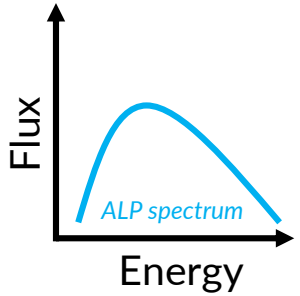

- **Motivation:** ALPs are theorized to have a unique spectral signature in the spectrum of a long GRB. No other known physical processes are predicted to produce such signature.

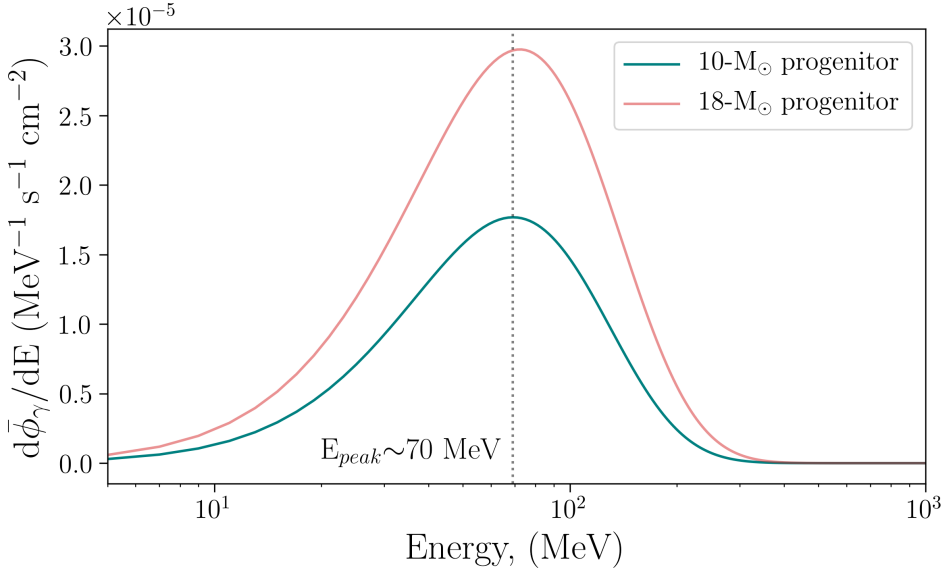

The observed ALP-induced gamma-ray spectrum for 10 and 18-M$_\odot$ progenitors averaged over 10 seconds.

MOTIVATION AND ASSUMPTIONS

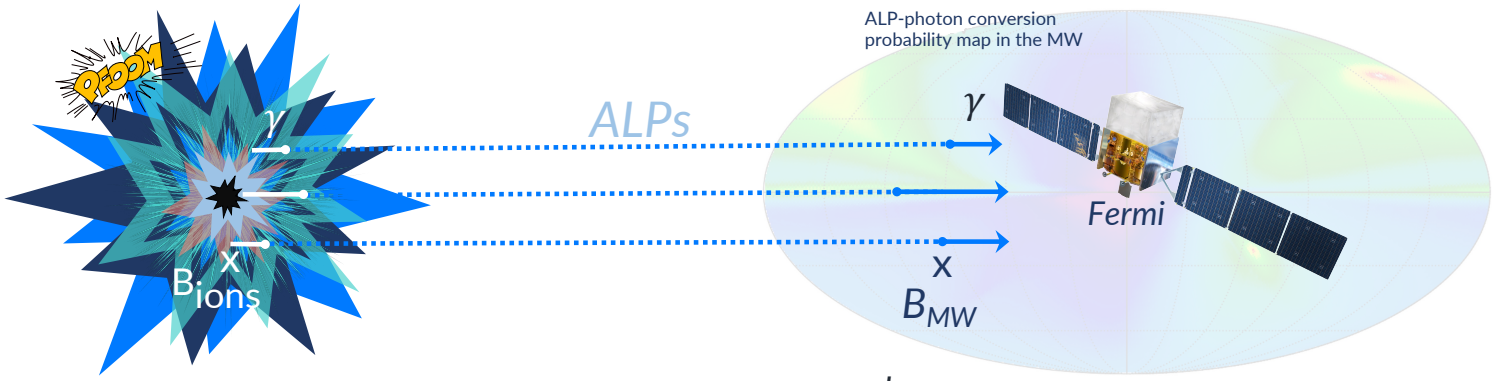

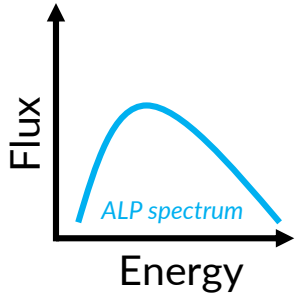

- **Motivation:** ALPs are theorized to have a unique spectral signature in the spectrum of a long GRB. No other known physical processes are predicted to produce such signature.
- **Assumptions:**

magnetic fields: only considering the MW magnetic field, neglecting IGMF

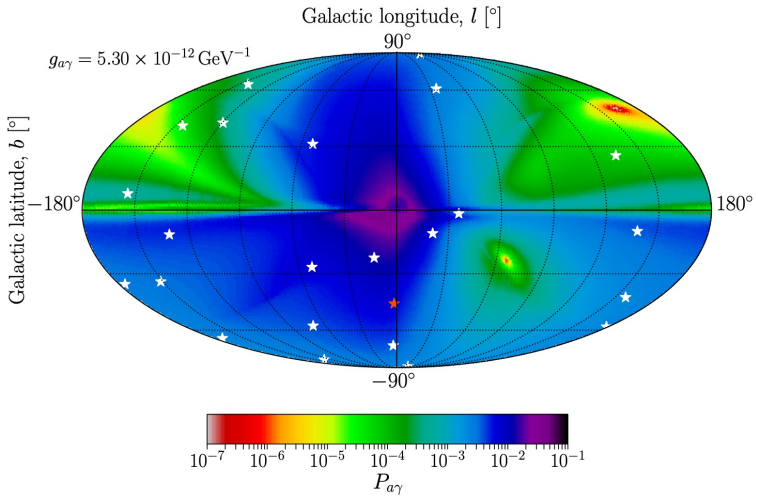

ALP-photon conversion probability map in the Milky Way's magnetic field.

ALP spectrum

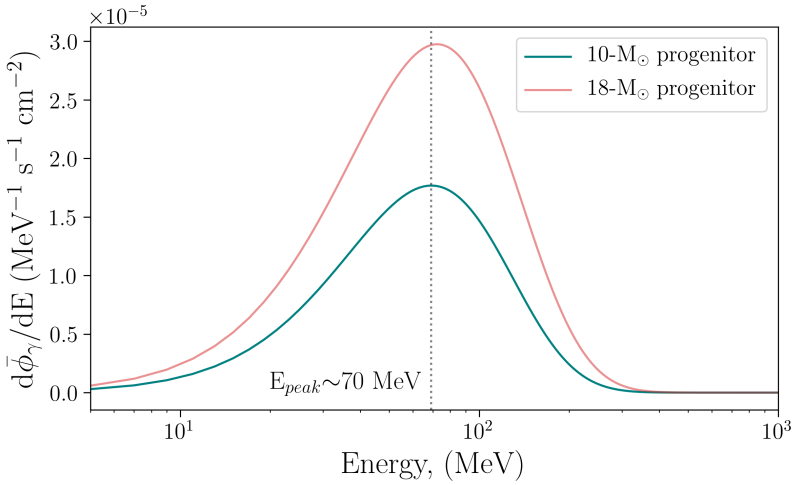

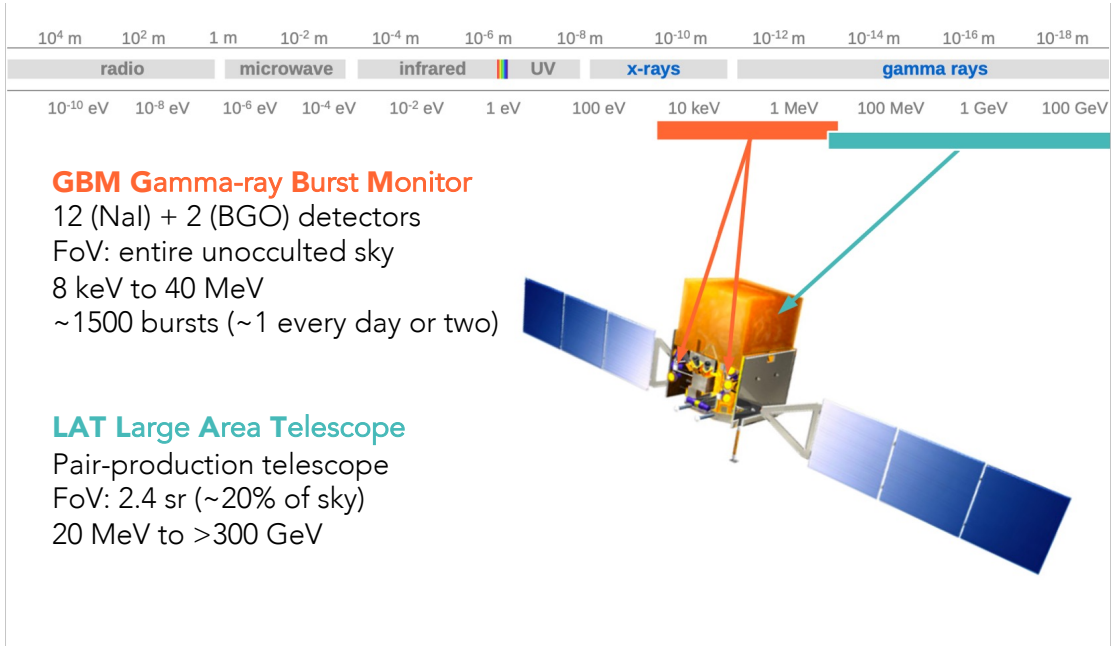

GBM Gamma-ray Burst Monitor
12 (NaI) + 2 (BGO) detectors
FoV: entire unocculted sky
8 keV to 40 MeV
~1500 bursts (~1 every day or two)

LAT Large Area Telescope
Pair-production telescope
FoV: 2.4 sr (~20% of sky)
20 MeV to >300 GeV

ALP spectrum

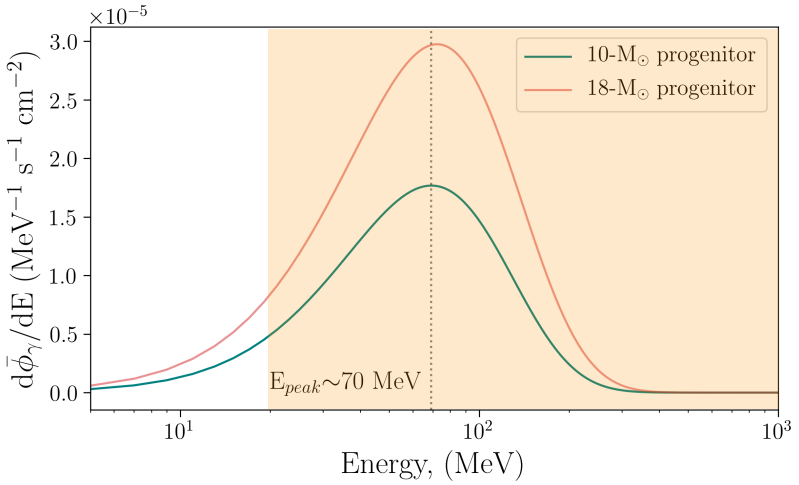

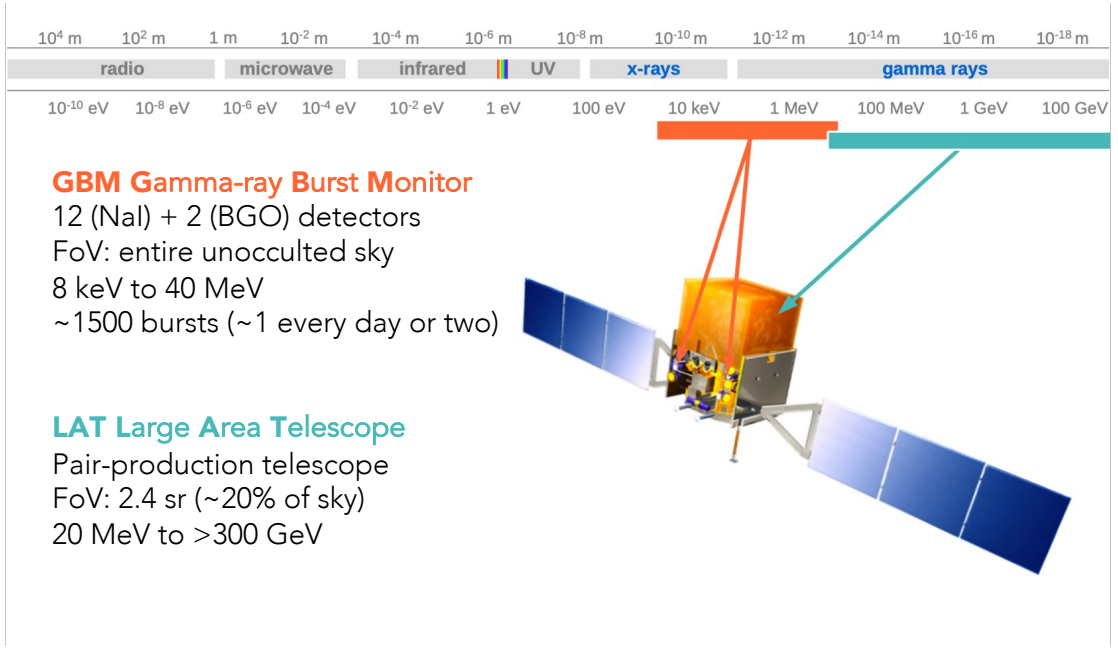

GBM Gamma-ray Burst Monitor
12 (NaI) + 2 (BGO) detectors
FoV: entire unocculted sky
8 keV to 40 MeV
~1500 bursts (~1 every day or two)

LAT Large Area Telescope
Pair-production telescope
FoV: 2.4 sr (~20% of sky)
20 MeV to >300 GeV

ALP spectrum

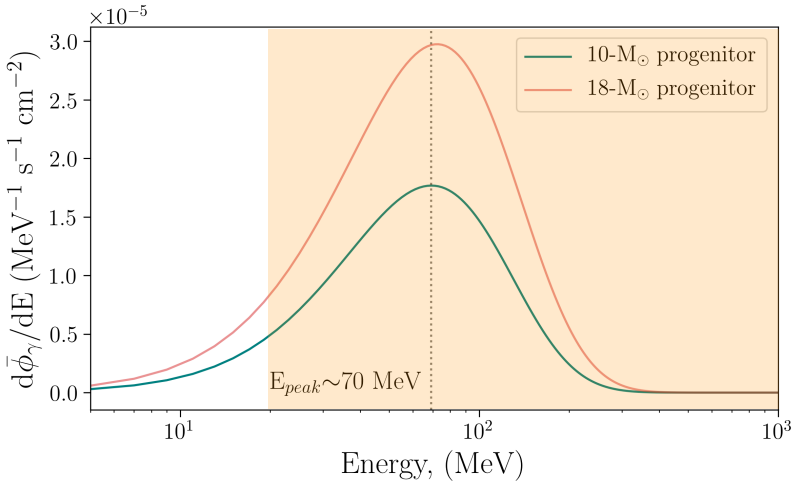

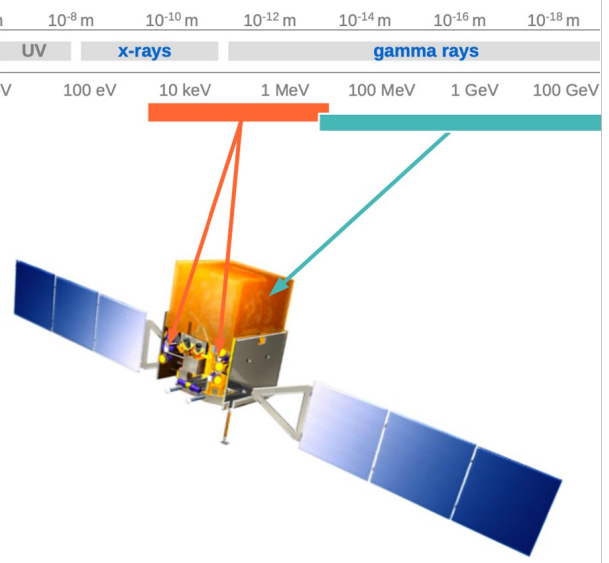

GBM Gamma-ray Burst Monitor
12 (NaI) + 2 (BGO) detectors
FoV: entire unocculted sky
8 keV to 40 MeV
~1500 bursts (~1 every day or two)

LAT Large Area Telescope
Pair-production telescope
FoV: 2.4 sr (~20% of sky)
20 MeV to >300 GeV

LAT LOW ENERGY (LLE) TECHNIQUE

- Standard LAT analysis: >100 MeV (Meyer et al. 2020). LLE analysis: >30 MeV
- Goal: maximizing the effective area of the LAT instrument in the low-energy regime
  - Relaxing requirements on the background rejection: more signal, but also more background!
  - Only works for pulse-like sources (i.e., transients)
  - Direction information necessary
  - Additional response functions needed (Monte Carlo simulations of a bright point source at the position of interest)
- Systematics: flux values on average lower than those from the standard LAT analysis

SENSITIVITY TESTING: ANALYSIS & RESULTS

Model backgrounds from the considered LLE-detected GRB sample.

Find the min, max, and median background levels.

Produce ALP signal normalized by a value from the normalization grid for 10-and 18-solar-mass progenitors.

Produce 2000 realizations of the backround+ALP spectrum and their corresponding (GRB) response functions (XSPEC fakeit function.)

Fit the ALP and the "background-only" model. Apply Wilks' Theorem and LLR test to fins for which normalization ALP model is preferred.

Find the coupling-distance parameter space for that normalization.

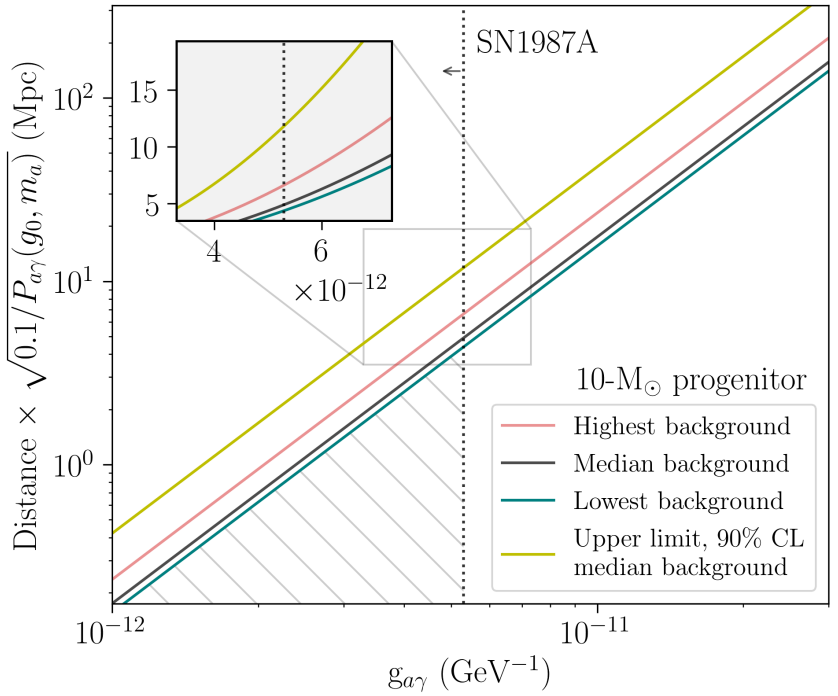

$N \propto 1/d^2$

Background level	Conversion probability, $P_\gamma(g_0)$	Distance limit (Mpc) 10 M$_\odot$	18 M$_\odot$
Low	0.1	4.4	6.5
Median	0.1	4.9	7.1
High	0.1	6.6	9.7
Low	0.05	3.1	4.6
Median	0.05	3.5	5.0
High	0.05	4.7	6.9
Low	0.01	1.4	2.1
Median	0.01	1.5	2.3
High	0.01	2.1	3.1
Low	0.001	0.4	0.7
Median	0.001	0.5	0.7
High	0.001	0.7	1.0

Crnogorčević et al. 2021 (PRD, arXiv:2109.05790)

SENSITIVITY TESTING: ANALYSIS & RESULTS

Model backgrounds from the considered LLE-detected GRB sample.

Find the min, max, and median background levels.

Produce ALP signal normalized by a value from the normalization grid for 10-and 18-solar-mass progenitors.

Produce 2000 realizations of the backround+ALP spectrum and their corresponding (GRB) response functions (XSPEC fakeit function.)

Fit the ALP and the "background-only" model. Apply Wilks' Theorem and LLR test to fins for which normalization ALP model is preferred.

Find the coupling-distance parameter space for that normalization.

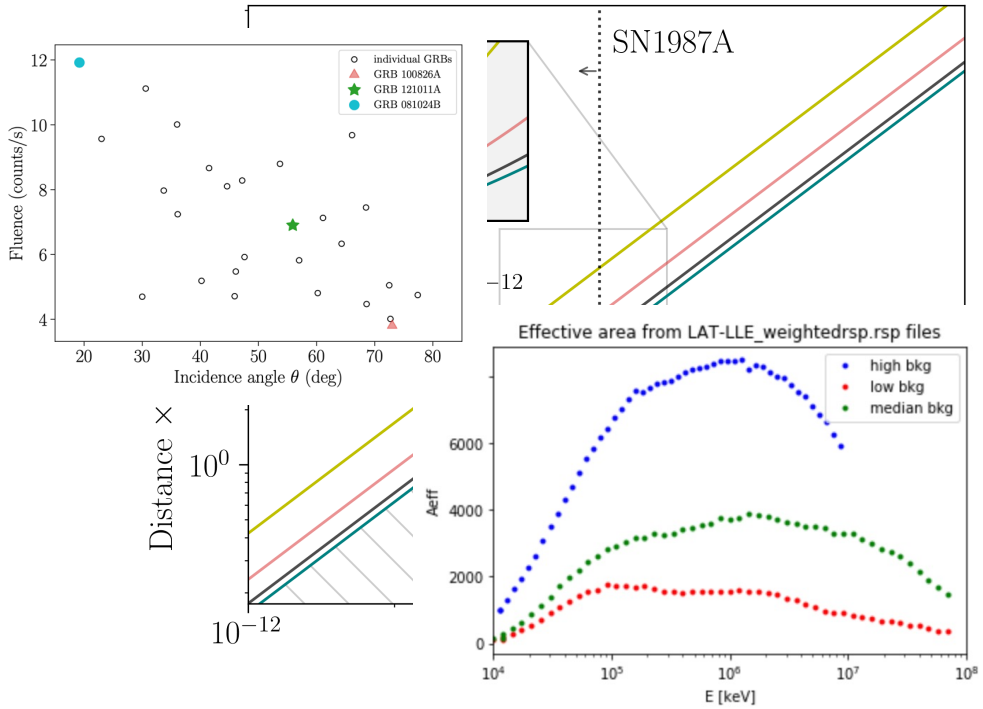

Background level	Conversion probability, $P_\gamma(g_0)$	Distance limit (Mpc) 10 $M_\odot$	18 $M_\odot$
Low	0.1	4.4	6.5
Median	0.1	4.9	7.1
High	0.1	6.6	9.7
Low	0.05	3.1	4.6
Median	0.05	3.5	5.0
High	0.05	4.7	6.9
Low	0.01	1.4	2.1
Median	0.01	1.5	2.3
High	0.01	2.1	3.1
Low	0.001	0.4	0.7
Median	0.001	0.5	0.7
High	0.001	0.7	1.0

Crnogorčević et al. 2021 (PRD, arXiv:2109.05790)

ADDITIONAL CONSIDERATION

Additional considerations: All-sky Medium Energy Gamma-ray Observatory (AMEGO) sensitivity analysis; motivation outlined the Snowmass 2021 Letter of Interest (Prescod-Weinstein et al. 2021, incl. Crnogorčević)

Quick factsheet about AMEGO:

- Probe-class mission concept
- High-sensitivity (200 keV – 10 GeV)
- Wide FoV, good spectral resolution, polarization
- Multimessenger astronomy (NS mergers, SNe, AGN)
- Order-of-magnitude improvement compared to previous MeV missions

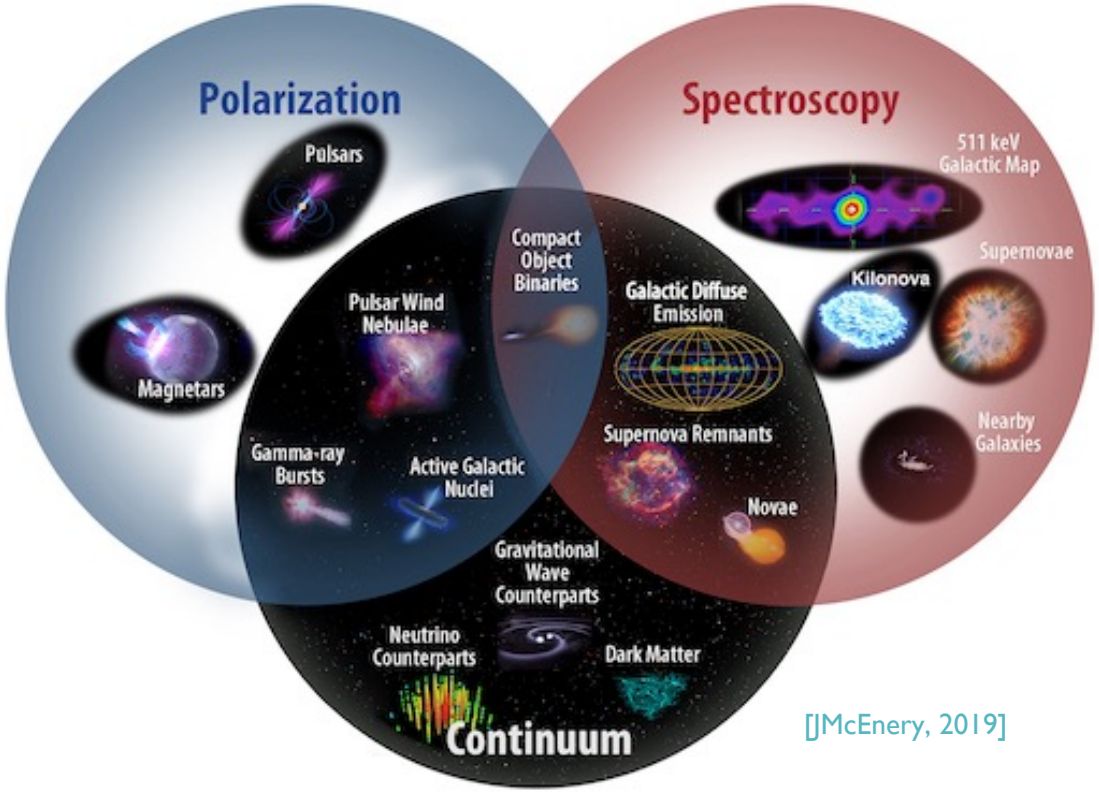

[JMcEnery, 2019]

ADDITIONAL CONSIDERATION

Additional considerations: All-sky Medium Energy Gamma-ray Observatory (AMEGO) sensitivity analysis; motivation outlined the Snowmass 2021 Letter of Interest (Prescod-Weinstein et al. 2021, incl. Crnogorčević)

Quick factsheet about AMEGO:

- Probe-class mission concept
- High-sensitivity (200 keV – 10 GeV)
- Wide FoV, good spectral resolution, polarization
- Multimessenger astronomy (NS mergers, SNe, AGN)
- Order-of-magnitude improvement compared to previous MeV missions

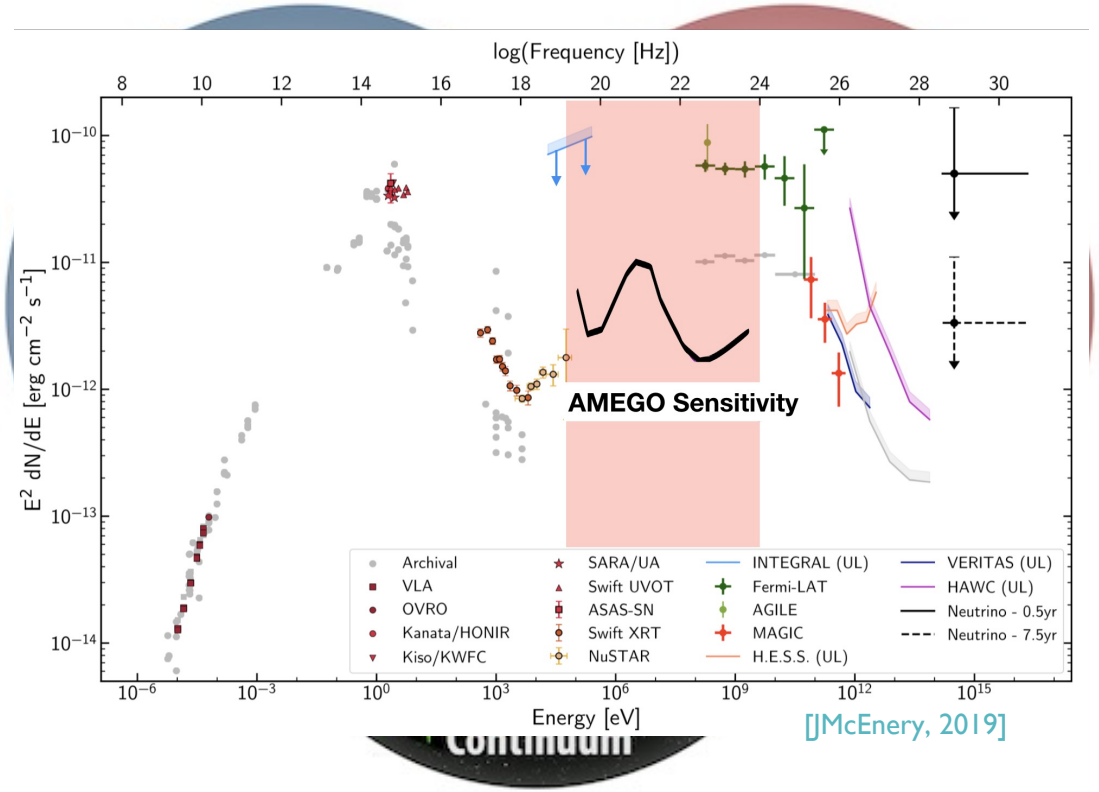

[JMcEnery, 2019]

ADDITIONAL CONSIDERATION

Additional considerations: All-sky Medium Energy Gamma-ray Observatory (AMEGO) sensitivity analysis; motivation outlined the Snowmass 2021 Letter of Interest (Prescod-Weinstein et al. 2021, incl. Crnogorčević)

- For a 10-solar mass progenitor, and background levels comparable to LAT in the low-energy regime:

Distance limit

improved by a factor of 5!

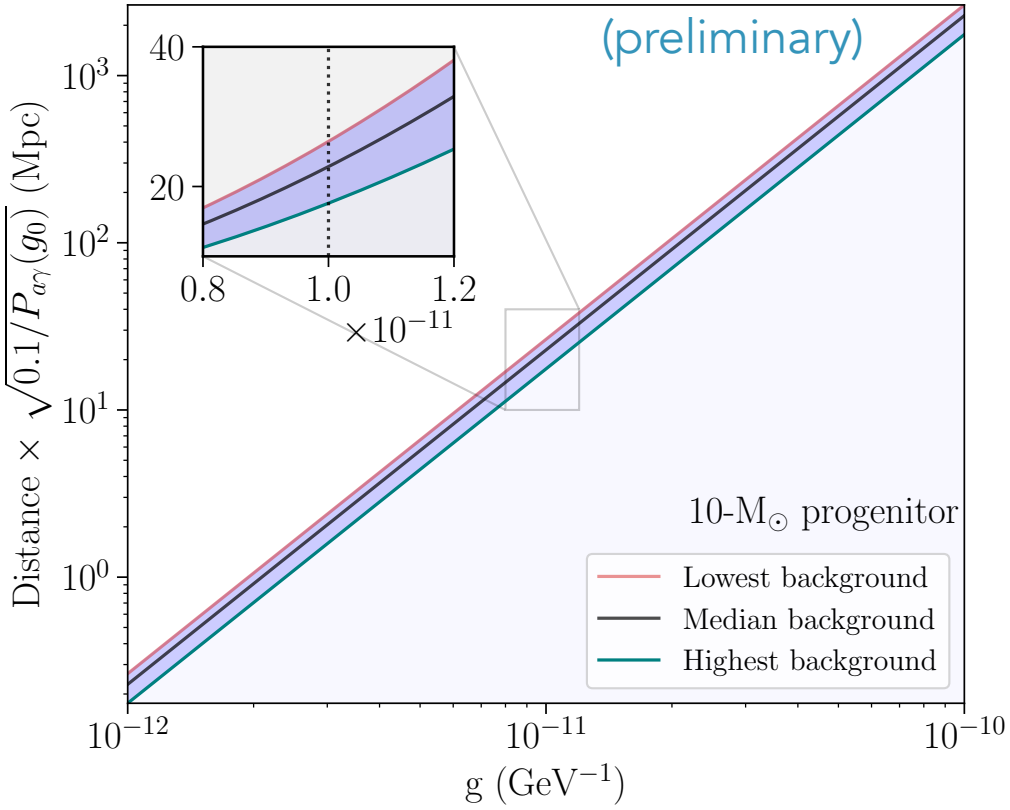

ADDITIONAL CONSIDERATIO

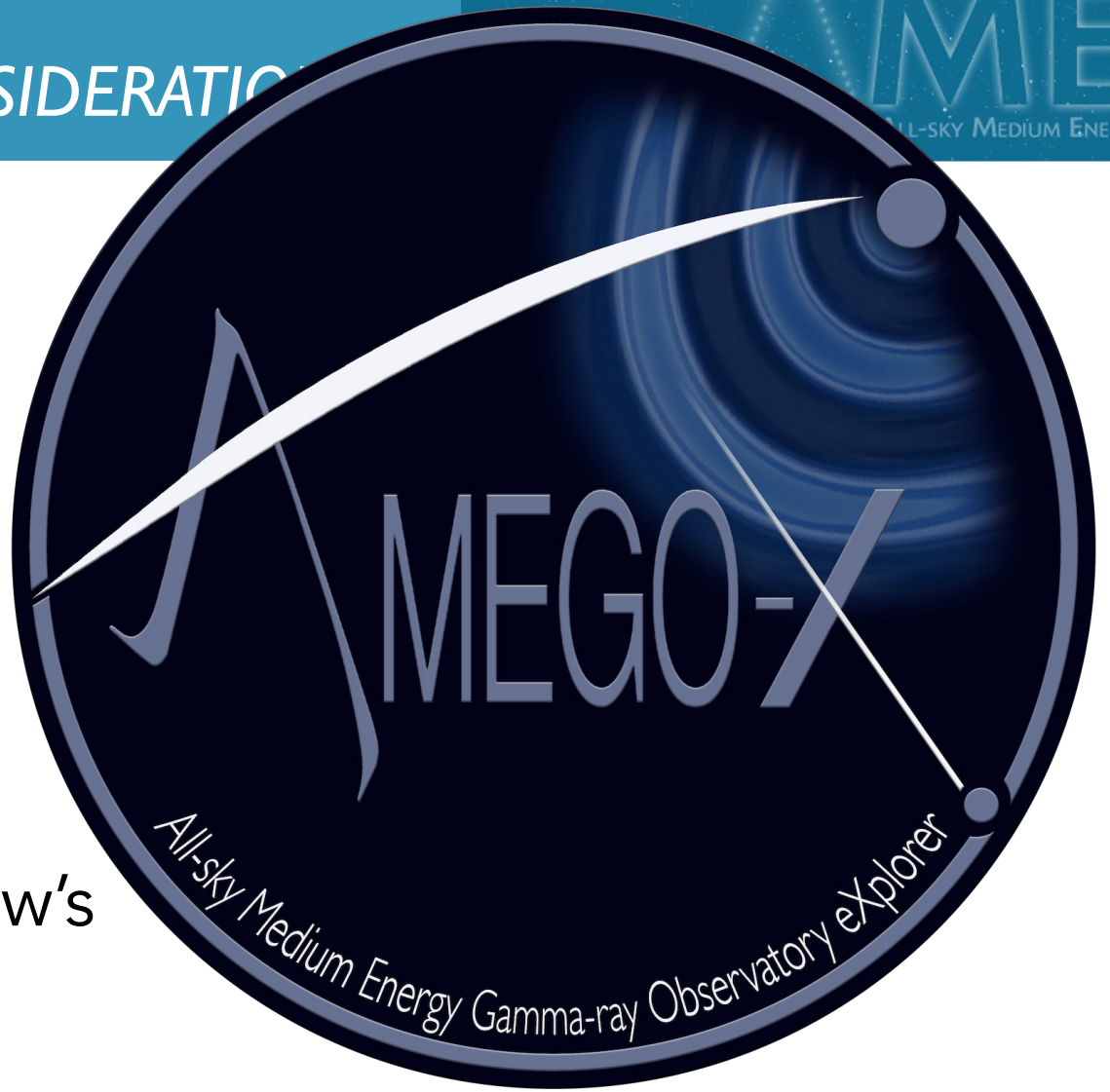

J. Perkins, tomorrow's plenary

MOTIVATION AND ASSUMPTIONS

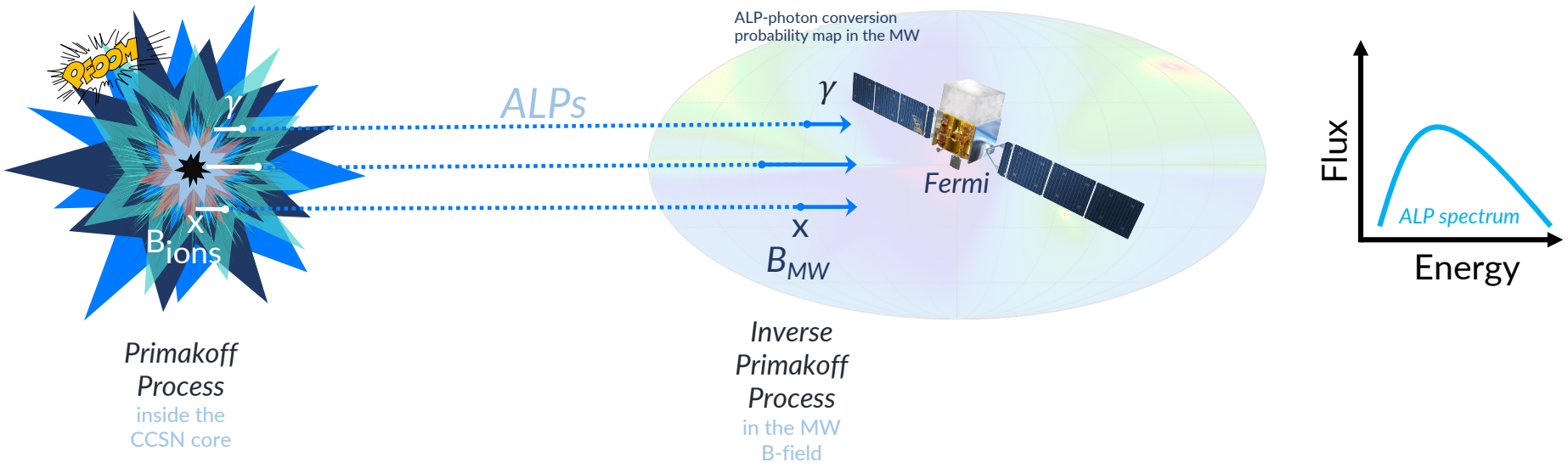

CCSNe → long Gamma-ray Bursts (GRBs)

GRB ANALYSIS

Property	Selection Criterion
Distance	unassociated (no redshift)
Detection significance	$\geq 5\sigma$ in LAT-LLE ($\gtrsim 30$ MeV)
Observed time interval	$\geq$ duration of the burst
Burst duration	long GRBs ($T_{95} \gtrsim 2$ seconds)

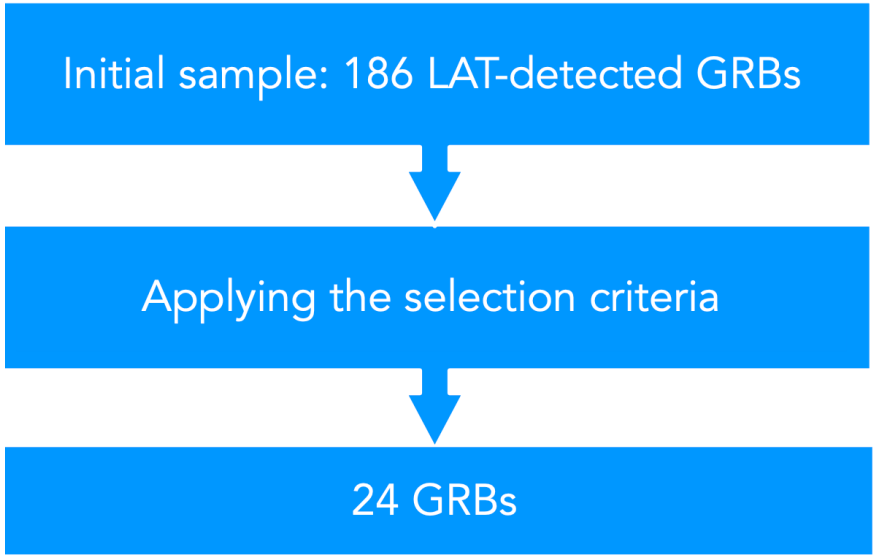

GRB ANALYSIS RESULTS

			grbm parameters			
GRB	T_{95} (s)	Best model(no ALP)	α_1	α_2	E_c (keV)	LLR
080825C	22.2	grbm	$-0.65^{+0.05}_{-0.05}$	$-2.41^{+0.04}_{-0.04}$	143^{+13}_{-12}	0.2
090217	34.1	grbm	$-1.11^{+0.04}_{-0.04}$	$-2.43^{+0.03}_{-0.04}$	16^{+13}_{-8}	0.1
100225A	12.7	grbm	$-0.50^{+0.25}_{-0.21}$	$-2.28^{+0.07}_{-0.09}$	223^{+112}_{-68}	0.0
100826A	93.7	grbm+bb	$-1.02^{+0.04}_{-0.04}$	$-2.30^{+0.03}_{-0.04}$	484^{+72}_{-63}	0.0
101123A	145.4	grbm+cutoffpl	$-1.00^{+0.07}_{-0.08}$	$-1.94^{+0.15}_{-0.12}$	187^{+74}_{-62}	5.8
110721A	21.8	grbm+bb	$-1.24^{+0.02}_{-0.01}$	$-2.29^{+0.03}_{-0.03}$	1000^{+28}_{-39}	0.0
120328B	33.5	grbm+cutoffpl	$-0.67^{+0.06}_{-0.05}$	$-2.26^{+0.05}_{-0.05}$	101^{+12}_{-13}	0.0
120911B	69.0	grbm	$-2.50^{+0.92}_{-1.04}$	$-1.05^{+0.63}_{-0.38}$	11^{+10}_{-2}	0.0
121011A	66.8	grbm	$-1.08^{+0.10}_{-0.21}$	$-2.18^{+0.11}_{-0.16}$	997^{+84}_{-26}	0.0
121225B	68.0	grbm	$-2.38^{+1.02}_{-0.40}$	$-2.45^{+0.06}_{-0.07}$	11^{+89}_{-3}	0.0
130305A	26.9	grbm	$-0.76^{+0.03}_{-0.03}$	$-2.63^{+0.06}_{-0.06}$	665^{+61}_{-55}	0.0
131014A	4.2	grbm	$-0.55^{+0.33}_{-0.98}$	$-2.65^{+0.17}_{-0.19}$	255^{+36}_{-11}	0.63
131216A	19.3	grbm+cutoffpl	$-0.46^{+0.28}_{-0.24}$	$-2.67^{+1.94}_{-0.94}$	178^{+77}_{-92}	0.0
140102A	4.1	grbm+bb	$-1.10^{+0.12}_{-0.09}$	$-2.41^{+0.16}_{-0.11}$	206^{+65}_{-92}	2.3
140110A	9.2	grbm	$-2.49^{+1.64}_{-1.59}$	$-2.19^{+0.20}_{-0.22}$	11^{+23}_{-3}	0.0
141207A	22.3	grbm+bb	$-1.21^{+0.09}_{-0.06}$	$-2.33^{+0.11}_{-0.13}$	999^{+18}_{-70}	0.0
141222A	2.8	grbm+pow	$-1.57^{+0.03}_{-0.02}$	$-2.83^{+0.46}_{-1.74}$	9971^{+390}_{-832}	0.0
150210A	31.3	grbm+pow	$-0.52^{+0.04}_{-0.05}$	$-2.91^{+0.11}_{-0.38}$	1000^{+517}_{-234}	0.0
150416A	33.8	grbm	$-1.18^{+0.04}_{-0.04}$	$-2.36^{+0.13}_{-0.21}$	999^{+187}_{-269}	0.0
150820A	5.1	grbm	$-0.99^{+0.56}_{-1.30}$	$-2.01^{+0.82}_{-0.27}$	303^{+61}_{-39}	0.0
151006A	95.0	grbm	$-1.35^{+0.06}_{-0.03}$	$-2.24^{+0.07}_{-0.08}$	998^{+33}_{-84}	0.0
160709A	5.4	grbm+cutoffpl	$-1.44^{+0.18}_{-0.12}$	$-2.18^{+0.15}_{-0.18}$	9940^{+373}_{-511}	1.0
160917A	19.2	grbm+bb	$-0.78^{+3.45}_{-1.40}$	$-2.39^{+0.20}_{-0.10}$	994^{+634}_{-216}	0.9
170115B	44.8	grbm	$-0.80^{+0.02}_{-0.04}$	$-3.00^{+0.10}_{-0.07}$	1000^{+226}_{-106}	2.8

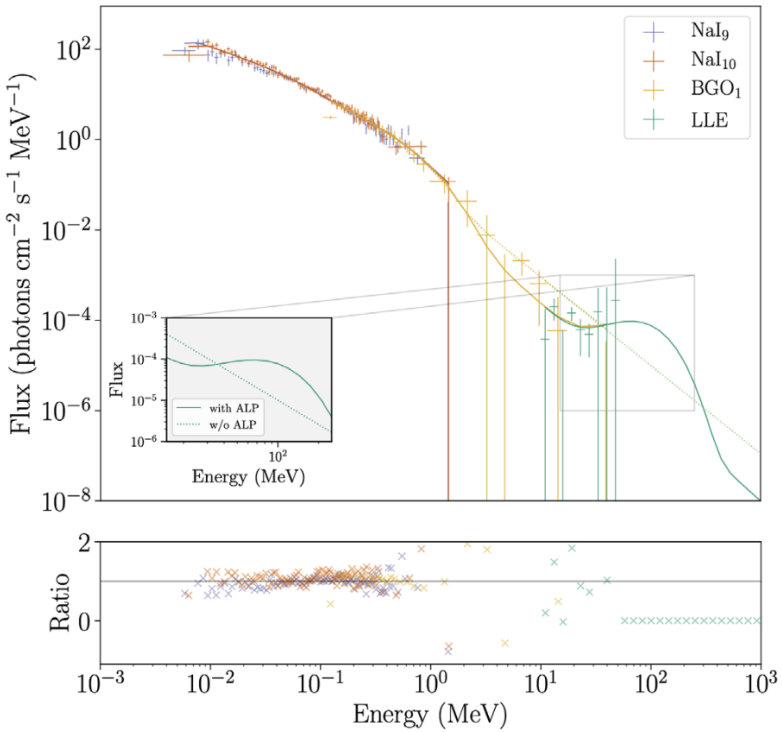

global p-value of ~0.3, indicating that this observation is not statistically significant.

CONCLUSIONS

- **Tools:** a developed pipeline for calculating distance limits for the current and future gamma-ray instruments for the given ALP mass and coupling
- **Novel results:** using a transient data class as observed by *Fermi* to probe its sensitivity. Results are consistent with the analysis using the standard LAT data [Meyer et al. 2016].
- **Good scientific case for the future instruments:** they need more sensitivity in the MeV region in order to be able to increase the statistics of sources considered
- **GRBs:** No statistically significant ALP detection in our LLE GRB sample.

SNEAK PEAK: WHEN TO SEARCH FOR ALPs?

- **The ALP signal should be coincident with the neutrino emission from a supernova**

→ For extragalactic SN, no neutrino signal is expected current generation of neutrino detectors [Kistler et al. 2011]; in the Milky Way ~2-3 SNe/century [Türler et al. 2006)

- **We can use optical light curves of extragalactic SNe to determine explosion times**

→ Method introduced in [Cowen et al. 2010] and applied in the context of ALP searches in [Meyer et al. 2020], resulting in most stringent upper limits on the light ALP parameter space

- **We can look for an ALP signal at the time of GRB emission, assuming that the GRB is ALP-induced**

→ Method introduced in [Crnogorčević et al. 2021] using a sample of LAT-detected GRBs. No significant (5 σ) detections reported

→ A study of GBM/LAT bursts with precursor emission: a systematic search for ALP excess in targeted time windows *before* presumed gamma-ray jet emission

Fermi GI Cycle 15 (PI: Crnogorčević)

BACK-UP SLIDES

LAT SENSITIVITY + EFFECTIVE AREA

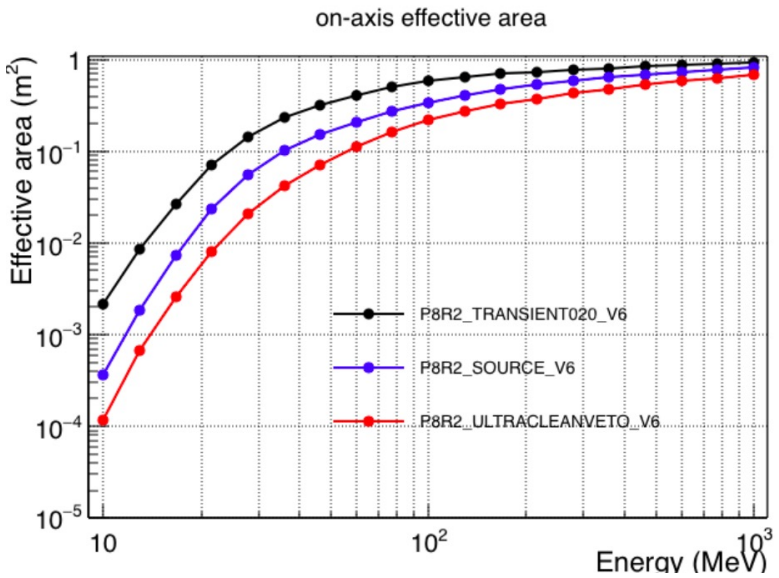

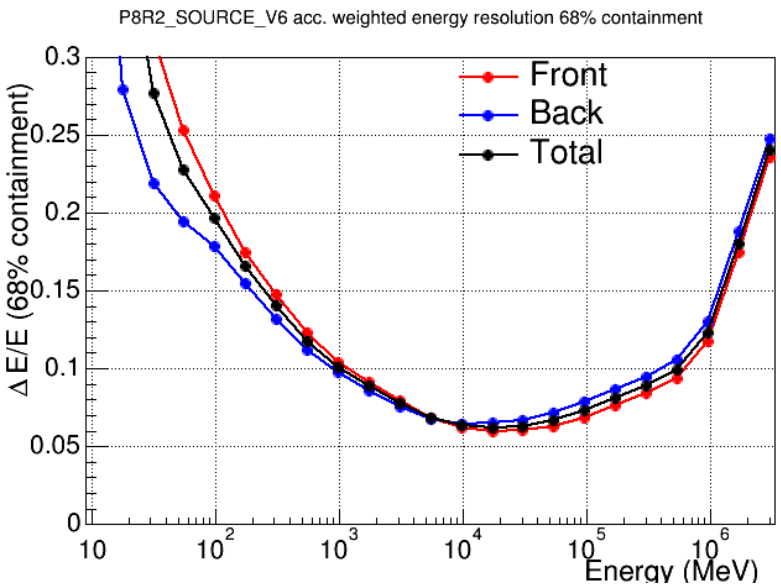

SN RATE AS A FUNCTION OF COMOVING DISTANCE

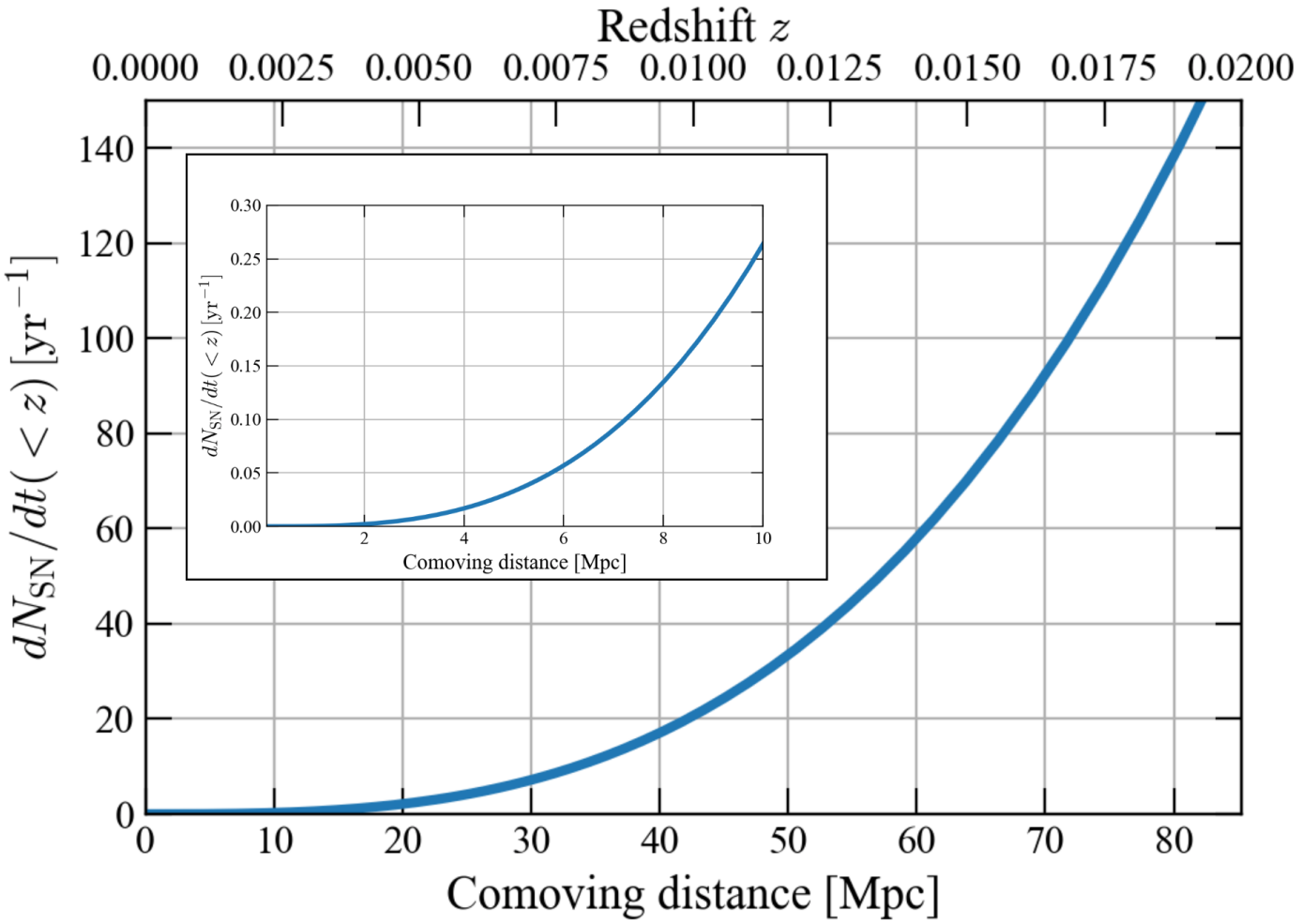

- SN Rate: ~ 150 yr^{-1} up to z = 0.02 (following Lien et al. 2009 with Salpeter IMF from Baldry et al. 2003 and cosmic SFR from Hopkins et al. 2006)
- Likely underestimated local SN rate by a factor of few (Ando et al. 2005, Kistler et al. 2013)
- No neutrino signal with the current generation of the neutrino detectors (Kistler et al. 2011)

GRB # AS A FUNCTION OF DISTANCE (CUMULATIVE FRACTION)

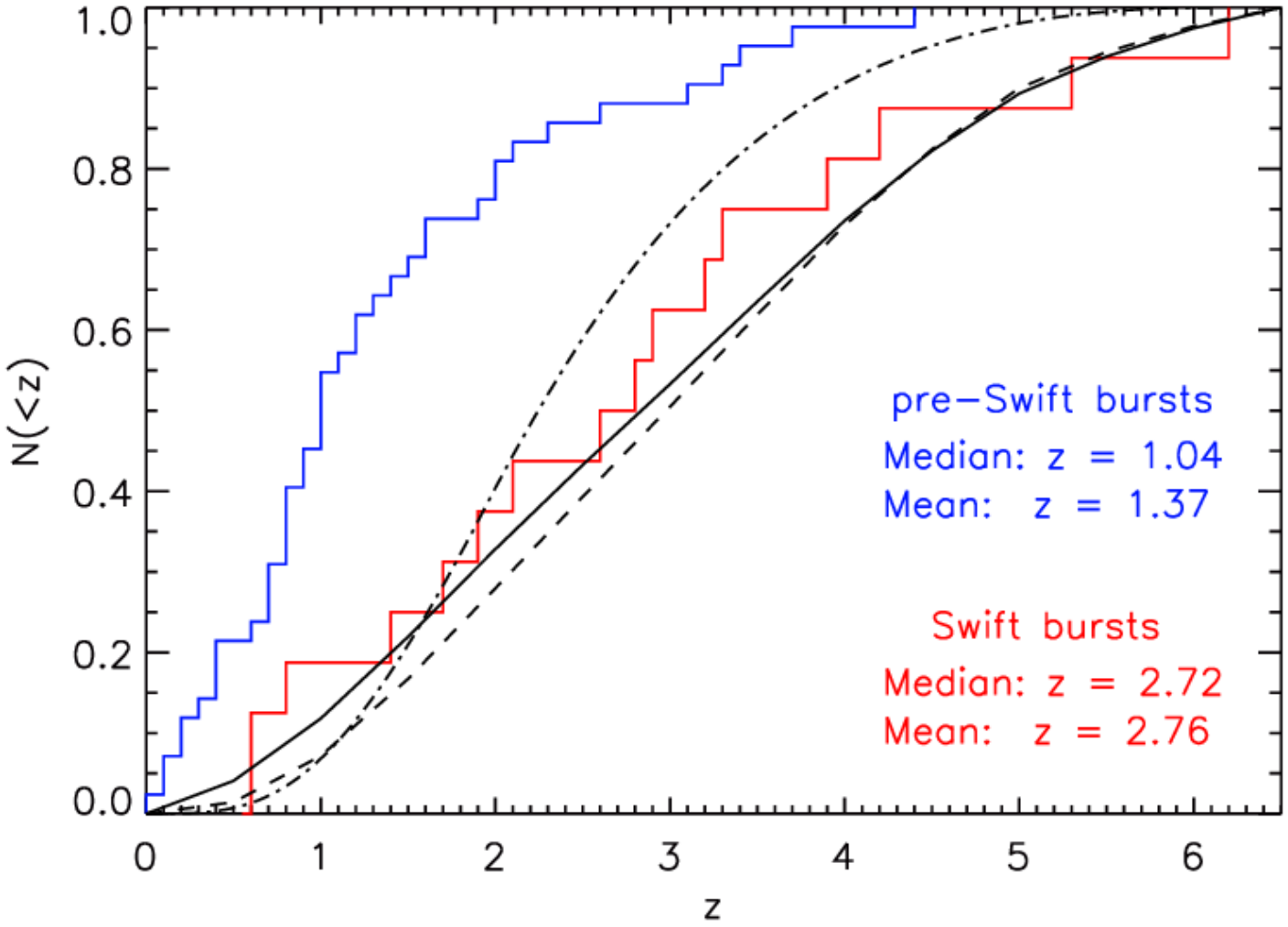

INTRODUCTION: THE DIFFERENCE BETWEEN AXIONS AND ALPS

- QCD axion: $m_a \sim 1/f_a$, where f_a is the energy breaking scale
- Axionlike particles: m_a and f_a are **independent parameters**
- Predicted in several **extensions** of the standard model (Majoron, Familon, String Theory…) [see Jaeckel & Ringwald 2010 for a review)
- Do **not solve** the strong CP problem

PRIMAKOFF RATE

2.2 Primakoff rate

ALPs coupled to the electromagnetic radiation as in Eq. (1.1) are produced in the stellar medium primarily through the Primakoff process [31], in which thermal photons are converted into ALPs in the electrostatic field of ions, electrons and protons.

Using the Heaviside–Lorentz convention for electromagnetism, the Primakoff conversion rate per unit time of photons into pseudoscalars is given by the following expression,

$$\Gamma = \frac{g_{a\gamma}^2\,\alpha\,n_p^{\rm eff}}{8}\left[\left(1+\frac{\kappa^2}{4E^2}\right)\ln\left(1+\frac{4E^2}{\kappa^2}\right)-1\right], \tag{2.1}$$

where α is the electromagnetic fine-structure constant, $n_p^{\rm eff}$ the effective number of targets, E the photon energy, and κ an appropriate screening scale which accounts for the finite range of the electric field of the charged particles in the stellar medium. This rate had been derived

Then, reduced Primakoff rate (taking into consideration all the assumptions about proton/electron degeneracy, reduction of the number of targets, reduction of proton mass):

$$\frac{d\dot{n}_a}{dE} = \frac{g_{a\gamma}^2\xi^2\,T^3\,E^2}{8\pi^3\left(e^{E/T}-1\right)}\left[\left(1+\frac{\xi^2T^2}{E^2}\right)\ln(1+E^2/\xi^2T^2)-1\right], \tag{2.7}$$

where

$$\xi^2 = \frac{\kappa^2}{4T^2}\,. \tag{2.8}$$

Then, integrate it over volume of the star to obtain the total number of ALPs (assumed 50 km, so that the accounted EOS holds

PRIMAKOFF RATE (CONT.)

And, the final curve can be fit by…

An excellent fit to the total production rate is provided by the following expression [32], also widely used in SN neutrino studies,

$$\frac{d\dot{N}_a}{dE} = C\left(\frac{E}{E_0}\right)^{\beta} e^{-(\beta+1)E/E_0} \quad . \tag{2.11}$$

Here C is a normalization constant while the fit parameter E_0 coincides with the average energy $\langle E_a \rangle = E_0$. Numerically, we find $C = 1.03\times10^{52}$ MeV^{-1} s^{-1}, $E_0 = 105.6$ MeV, $\beta = 2.145$ for the curve corresponding to $t = 1$ s shown in Fig. 4. Similarly, we document for future use

Now, if we are interested in the differential ALP flux per unit energy at Earth, since the emission is necessarily isotropic in our model, we should simply consider

$$\frac{d\Phi_a}{dE} = \frac{1}{4\pi d^2}\frac{d\dot{N}_a}{dE} , \tag{2.12}$$

with d the distance to the supernova, which is 50 kpc in our case (1 kpc $= 3.086 \times 10^{21}$ cm).

CONVERSION PROBABILITY VS ENERGY

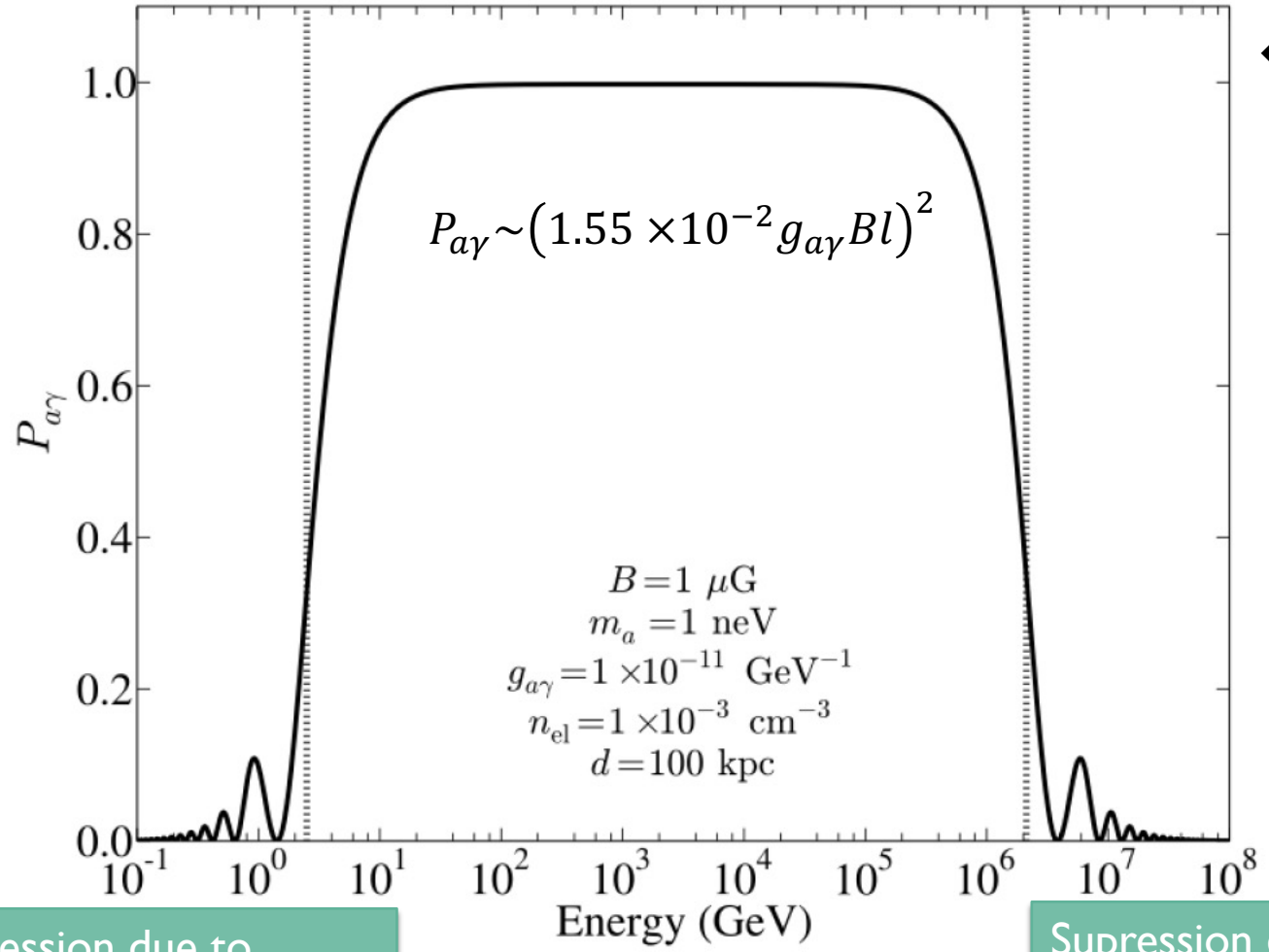

← In a coherent magnetic field

→ Strong mixing regime:
e.g. intergalactic magnetic field:
$B \sim 1$ nG,
$g_{a\gamma} \sim 10^{-11}$ GeV^{-1},
distance 5 Mpc

$$O\left(P_{a\gamma}\right) \sim 10^{-3}$$

Supression due to momentum mismatch because of non-zero ALP mass.

Supression due to photon-photon dispersion with external magnetic field and background radiation fields (CMB)

[Dobrynina et al. 2015]

SN1987A

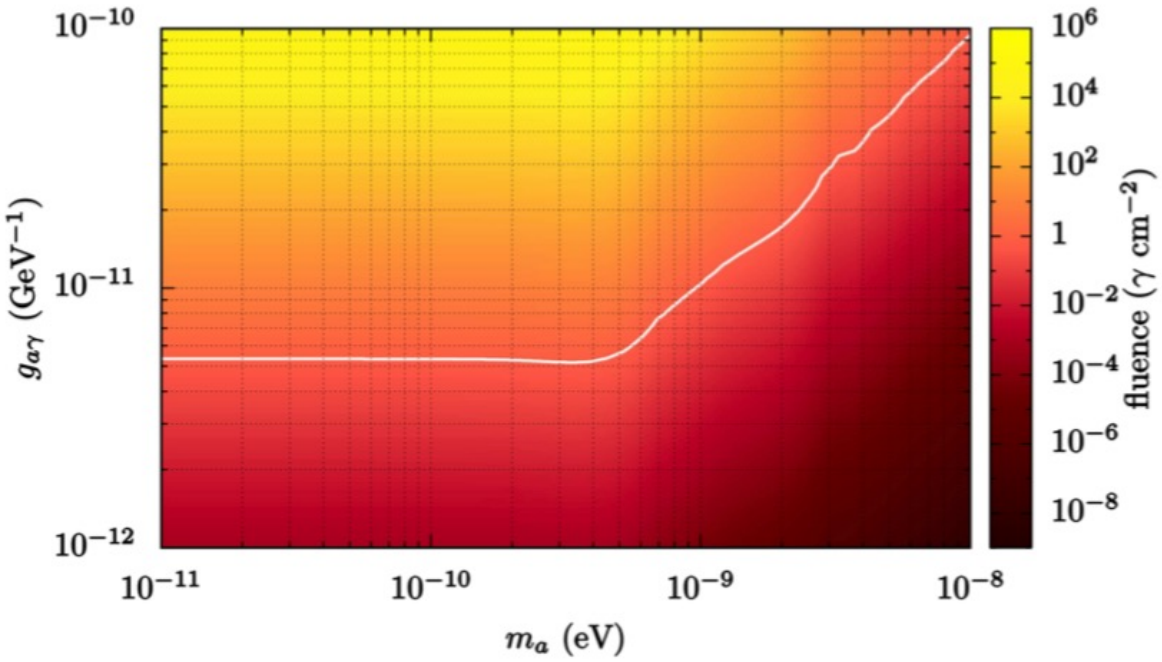

SN1987A fluence for a given coupling rate and the ALP mass. Stable upper bound: $g_{a\gamma} = 5.3 \times 10^{-12}$ GeV^{-1} and
$m_a = 4.4 \times 10^{-10}$ eV.

WILKS' THEOREM

$$D = -2 \ln \left(\frac{\text{likelihood for null model}}{\text{likelihood for alternative model}} \right)$$

- For large N_{tot} we can apply Wilks theorem and assume that the background distribution follows a χ^2_1 distribution.

$$p - \text{value} = \int_{\lambda_{\text{obs}}}^{\infty} \mathrm{d}x \chi^2_k(x) = 1 - \text{erf}(\sqrt{\lambda_{\text{obs}}/2})$$

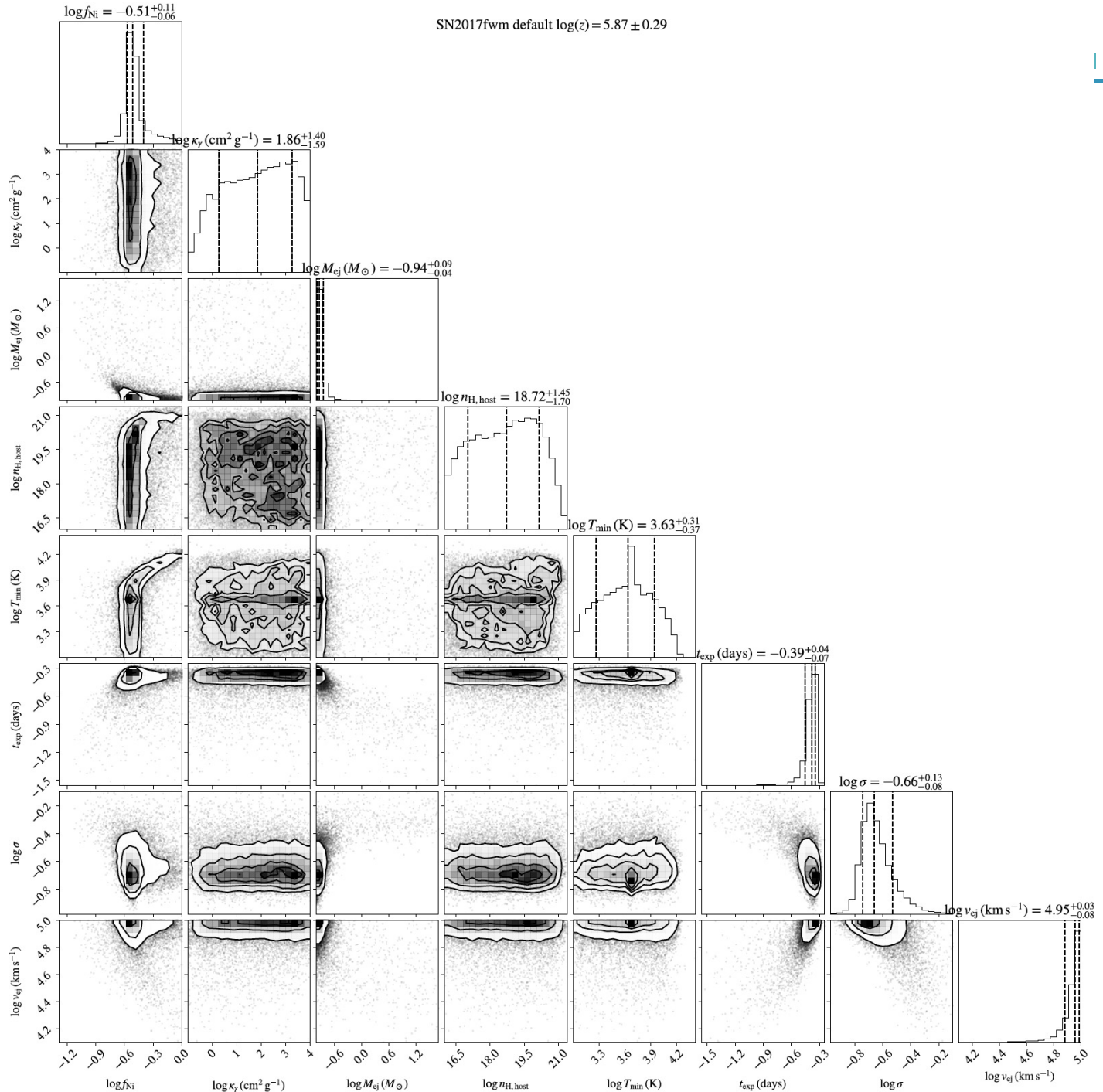

BACK-UP: OPTICAL LIGHTCURVES & EXPLOSION DETERMINATION